

Non-magnetic spin generation in n-doped GaAs quantum wells

L. Jiang^{1,2}, M. Q. Wang² and M. W. Wu^{1,2},¹Hefei National Laboratory for Physical Sciences at Microscale,

University of Science and Technology of China, Hefei, Anhui, 230026, China

²Department of Physics, University of Science and Technology of China, Hefei, Anhui, 230026, China^y

(Dated: October 25, 2019)

We demonstrate that the spin polarization/current can be generated non-magnetically in two-terminal semiconductor quantum well structures with linear momentum-dependent spin-orbit coupling and charge density gradient at high temperature. The induced spin polarization/current is not only restricted in the region with charge gradient but can be further transferred to the region with uniform charge density. This provides a novel scheme to build devices that can produce and inject large spin polarization pure electrically. We show that the spin generation and injection is very robust in practical devices.

PACS numbers: 72.25.Pn, 72.25.Mk, 72.25.Dc, 67.57.Lm, 72.25.Rb

The growing field of spintronics which tries to design devices that integrate the spin degree of freedom to the traditional electronic devices has attracted much attention [1, 2]. A fundamental obstacle in semiconductor spintronics is the efficiency of generation and detection of the spin polarized carriers in semiconductors. In addition to various proposals of optical pumping and spin injection from ferromagnetic metals or semiconductors, the non-magnetic spin generation and detection through electrical manner have attracted special attention. The spin-orbit coupling that bridges the spin precession and the spatial motion plays the central role in the pure electrical spin generation and detection as it can make the conversion between the carrier imbalance and the spin imbalance.

A charge current driven by the spin-orbit coupling and the asymmetric spin- β scattering in the presence of a uniform spin polarization has been observed by optical pumping in n-type GaAs quantum well (QW) structures [3, 4]. A similar result of the in-plane charge current induced by the vertical tunneling through a semiconductor barrier was predicted recently [5]. These spin-galvanic effects make it possible to design pure electrical spin detectors. The reverse to the above ideas is to design pure electrical spin generator that converts the charge current/accumulation to the spin current/accumulation. The recently discussed spin-Hall effect [6] is one example of the reversed spin-galvanic effect, although the robustness of the induced spin current is still under debate [7].

In this letter we propose a scheme of a pure electrical generation of the spin polarization in the present of a charge gradient through both the analytic solution of a highly simplified model and the numerical simulation of the full many-body kinetic transport equations. We show that a robust spin polarization/current can be induced in the designed doped QW structures of zinc-blend semiconductors. With this scheme we further demonstrate that a pure electrical spin injection can be easily achieved in practical semiconductor devices.

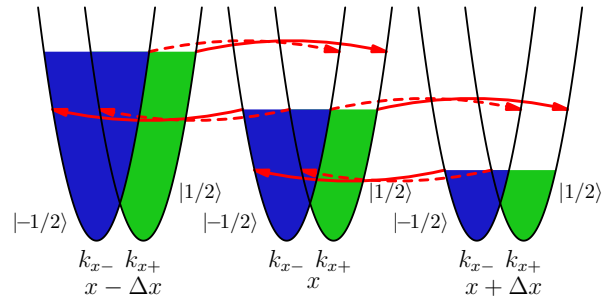


FIG. 1: Schematic of spin generation due to carrier density gradient along the x-axis. In the presence of the linear-momentum spin-orbit coupling, the bottom of the two spin bands are separated (the green one vs. the blue one in the figure). As a result, for forward direction ($k_x > 0$), the number of the carriers in $j=2i$ -band divides from left to right is larger than that in $j=1i$ -band (due to larger momentum of carriers in $j=2i$ -band). However, the backward direction ($k_x < 0$) of carriers from $j=2i$ -band is smaller than that from $j=1i$ -band. Therefore the system can induce a spin polarization. It is noted that the backward scattering of both spin bands experiences Pauli blocking due to the density gradient which further facilitates the spin pumping. In the figure the solid (dashed) arrows stand for larger (smaller) transfer rate.

The schematic of the pure electrical spin generation in the system with linear-momentum-dependent spin-orbit coupling is sketched in Fig. 1. Due to the coupling, the conduction band is split into two helix spin bands with spin $1=2$ in the direction depending on the carrier momentum (parallel to the momentum for the Dresselhaus term [8, 9] and perpendicular for the Rashba term [10]). The energy minima of the two spin bands locate at k_{x+} and k_x respectively and the Fermi wave-vectors of these two spin bands differ by $k_{x+} - k_x$. In the system with non-uniform spatial charge distribution, a current is presented due to the diffusion. If the two spin bands are in local equilibrium, the diffusion of the carriers with spin $1=2$ induces a current roughly proportional to $k_x dn(x)/dx$, with $n(x)$ standing for the carrier density

at x . The difference between these two currents consequently builds a net spin polarization at x , with the spin generation rate proportional to the difference between momentum shift of the two spin bands and the gradient of the spatial charge. In reality, there is spin relaxation that destroys the spin polarization. Consequently, spin polarization in the steady state should depend on the spin relaxation and can be estimated to be proportional to $\frac{1}{s} \ln(x) = dx$, in which s is the spin life time and α represents the strength of the spin-orbit coupling, by equaling the spin generation rate and the spin loss rate. It is further noted that the orientation of the induced spin polarization depends on the spin-orbit coupling mechanism. For Rashba spin-orbit coupling [10], when the QW momentum is along the z -axis, spins point to the y -axis for carriers traveling along the x -direction, and the induced spin polarization is along the y -axis. While for Dreselhaus spin-orbit coupling [8, 9], the induced spin polarized along the x -axis. Reversely, one can also obtain a charge gradient proportional to the spin-orbit coupling and spin polarization when the carriers are properly spin-polarized.

The generation of the spin polarization/current in the system with spin-orbit coupling and charge gradient can be studied rigorously in the framework of the kinetic Bloch equation approach [11, 12, 13], which takes into account the carrier (charge and spin) diffusion in the spatial non-uniform system, the carrier drift driven by the electric field, the spin precession around the D'yakonov and Perel' (DP) effective magnetic field [8, 14] and the mean magnetic field of the surrounding magnetic momentums of electrons, as well as the scattering. In n-type semiconductor QW's with the growth direction along the z -axis, the kinetic Bloch equations read [13]

$$\begin{aligned} \frac{\partial \langle R ; k ; t \rangle}{\partial t} &= \frac{1}{2} f_5 \langle R ; k ; t \rangle; \langle k ; R ; k ; t \rangle g \\ &+ \frac{1}{2} f_5 \langle R ; k ; t \rangle; \langle R ; k ; t \rangle g \frac{\partial \langle R ; k ; t \rangle}{\partial t} \\ &= \frac{\partial \langle R ; k ; t \rangle}{\partial t} ; \end{aligned} \quad (1)$$

in which $\langle R ; k ; t \rangle$ represents a single-particle density matrix. The diagonal elements $\langle R ; k ; t \rangle$ of $\langle R ; k ; t \rangle$ represent the electron distribution functions of electrons with 2D wave-vector $k = (k_x, k_y)$ and spin at position R and time t (Here i is the spin index in the lab coordinate instead of the helix spin index in Fig. 1.). The off-diagonal elements $\langle R ; k ; t \rangle$ are the inter-spin-band correlations. The quasi-particle energy spectrum $\pi(R ; k)$

is composed of

$$\begin{aligned} \pi(R ; k ; t) &= \frac{k^2}{2m} \alpha + h(k) \alpha = 2 \\ e(R ; t) \alpha &+ \alpha(R ; k ; t); \end{aligned} \quad (2)$$

with m standing for the effective mass and α representing the Pauli matrices. $h(k)$ is the effective magnetic field due to the DP spin-orbit coupling. In QW structure, $h(k)$ is usually composed of the Dresselhaus term [9] caused by the bulk inversion asymmetry and the Rashba term [10] caused by the structure inversion asymmetry.

$\langle R ; t \rangle$ is the electric potential which is determined by the Poisson equation,

$$\nabla^2 \langle R ; t \rangle = e[n(R ; t) - n_0(R)] = 0; \quad (3)$$

with $n(R ; t) = \int_k f(R ; t)$ and $n_0(R)$ denoting the carrier and the background charge densities respectively.

$\alpha(R ; k ; t)$ is the self-energy from the electron-electron interaction up to the Hartree-Fock (HF) order. The coherent term $\alpha(R ; k ; t) = \alpha_{tj}$ describes the spin precession around the DP effective magnetic field together with the mean magnetic field from the surrounding magnetic momentums of electrons, i.e., the HF term. The scattering term $\alpha(R ; k ; t) = \alpha_{tj}$ describes the scattering from electron-in-purity, electron-phonon and electron-electron Coulomb scattering. The expressions of the coherent and the scattering terms can be found in our previous work [15].

A greatly simplified analytic solution of the kinetic equations can be obtained when the spin-orbit coupling is weak by only considering the elastic scattering in $\alpha(R ; k ; t) = \alpha_{tj}$ and neglecting the coupling to the Poisson equation as well as the spin precession induced by the HF term. Similar to the approach used in the study of the spin relaxation due to the DP mechanism [16], one expands the quantities that depend on the wavevector $k = k(\cos \theta, \sin \theta)$ as summation of Fourier series of the angle. For example, the density matrix is expanded as

$$\langle R ; k ; t \rangle = \sum_{l=1}^{\infty} \langle R ; k ; t \rangle e^{i l \theta}; \quad (4)$$

in which l is an integer and $\langle R ; k ; t \rangle = \int_{R^2} e^{i l \theta} \langle R ; k ; t \rangle d\theta = 2$. Under the above mentioned approximation, one is able to write out the equations for the spin independent electron distribution function $f_0(R ; k ; t) = \text{Tr} \langle R ; k ; t \rangle g$ and the spin momentum $S_0(R ; k ; t) = \text{Tr} \langle R ; k ; t \rangle g$ as

$$\begin{aligned} \frac{\partial S_{0,i}(R ; k ; t)}{\partial t} &= \frac{k^2}{2m} \langle R ; k \rangle^2 r_R^2 S_{0,i}(R ; k ; t) - \frac{k \langle R ; k \rangle}{m} \text{Re} \left[\frac{h}{i} \langle R_x, i \langle R_y \rangle \rangle S_0(R ; k ; t) \right] + \frac{1}{4} \sum_{j=1}^i \langle R_j, \alpha_{R_j} \rangle f_0(R ; k ; t) \end{aligned}$$

$$+ 2 \cdot 1(R; k) R e \cdot 1(k) \cdot 1(k) S_0(R; k; t) + 2 \cdot 3(R; k) R e \cdot 1(k) \cdot 1(k) S_0(R; k; t) = 0; \quad (5)$$

$$\frac{\partial f_0(R; k; t)}{\partial t} - \frac{k^2 \cdot 1(R; k)}{2m} r_R^2 f_0(R; k; t) + \sum_{ij}^0 \partial_{R_i} S_{0;j}(R; k; t) = 0; \quad (6)$$

in which

$$\begin{matrix} 0 & k^2=2 & (=-a)^2 \\ 0 & 0 & 1 \\ 0 & k^2=2 & (=-a)^2 \\ 0 & 0 & 0 \end{matrix} \quad \begin{matrix} 0 & 1 \\ 0 & 0 \end{matrix}$$

$!_1(k) = k=2[(=-a)^2 k^2=4](1; i; 0) + k=2(i; 1; 0)$, and $!_3(k) = k=8(1; i; 0)$ with i standing for the Dreselhaus and Rashba spin-orbit coupling strengths and a being the width of the QW. $!_1(k) = R^2 W(k;) [l \cos(l)] d=2$ is the relaxation rate of the elastic scattering with $W(k;)$ standing for the elastic scattering cross section.

Equations (5) and (6) describe the transport of the spin and charge as well as the inter-conversion between the spin and charge gradient. Equation (5) shows the diffusion, generation and relaxation of the spin polarization: The second and the third terms of Eq. (5) are the diffusion of the spin signal due to the spatial inhomogeneity and the precession of the spin around the DPP effective magnetic field during the diffusion. The fourth term manifests the spin generation rate and is proportional to the spin-orbit coupling strength and the gradient of the charge density. The last two terms are nothing but the spin relaxation $S_{0;i}(R; k; t) = \frac{1}{s}(R; k)$ from the DPP mechanism [8, 14] with $\frac{1}{s}(R; k)$ representing the spin relaxation time along the i -axes. In the steady state of a system with a constant charge density gradient along the x -axis, one finds that only the last three terms in Eq. (5) survive to the leading order of the spin-orbit coupling strength and the spatial gradient. Therefore one obtains the spin polarization

$$S(x) = \frac{s(x)}{4} [k^2=2i (=-a)^2]; ; 0 \frac{dn(x)}{dx}; \quad (7)$$

with $s(x) = \int_R^R s(x; k) f_0(x; k) dk = f_0(x; k) dk$, the average spin relaxation time, and $hk^2 i = k^2 f_0(x; k) dk = f_0(x; k) dk$. This exactly agrees with what obtained above from the simple argument. The induced spin polarization is spatial uniform in the system with constant charge gradient and constant spin relaxation rate. As a result, the induced spin polarization does not undergo any diffusion. Once an electric field is applied, the polarized carriers are drifted and one obtains a spin current together with the charge current, both in the direction of the electric field.

It is of interest to note from Eq. (7) that a large spin S does not necessarily require a stronger spin-orbit coupling. Actually in the regime that the spin relaxation is dominated by the DPP mechanism, a system with small

spin-orbit coupling may result in a large spin polarization due to the faster increase of the spin relaxation time $s(x)$ which is proportional to $1=^2$ (or $1=^2$). Therefore S increases with the decrease of the coupling strength until the coupling strength is decreased so much that other spin relaxation mechanisms take over. Then one returns to the normally believed regime that stronger spin-orbit coupling strength gives larger spin polarization.

The above analysis shows the possibility of the generation of spin polarization/current from the charge gradient. However the efficiency of the effect in practical devices is left to be validated. In the following, we show the efficiency of the spin generation of a system with charge gradient by considering GaAs QW structures through numerical simulation. In the simulation, we self-consistently solve the kinetics Bloch equations Eq. (1) with the Dreselhaus spin-orbit coupling, the electron-electron HF contribution, as well as all the scattering, the electron-in purity, the electron-phonon and the electron-electron Coulomb scattering included, together with the Poisson equation Eq. (3). The numerical scheme is laid out in detail in [15] and the material parameters are taken from [17].

The charge gradient in semiconductors can be easily achieved and sustained through designed doping. In Fig. 2 we demonstrate the spin generation of a specially doped GaAs QW with well width $a = 5$ nm at 120 K. As shown in the figure, the uniform background positive charge density in region I is chosen to be 10^{12} cm^{-2} and it smoothly goes down to the uniform density 10^{11} cm^{-2} in region III over a small "transition" region II. In the simulation, the impurity density is set to the background positive charge density. It is seen that a stable spin polarization $P(x) = S_x(x) = n(x)$ is created in region II where the background charge density presents a gradient. Moreover the induced spin polarization is not only localized to region II, instead it peaks with a very large spin polarization (about 31 %) at the right edge of this region and extends to the regions where the charges are spatially uniform. The spin polarization outside region II extends up to 0.5 μm in the absence of electric field in region III, which is of the order of the spin injection length in GaAs QW under the condition we used. When an additional forward voltage of 0.33 V which creates an electric field of 2 kV/cm in region III is applied, the spin polarization is not destroyed. Instead, more spin polarization is driven to region III to create a larger spin injection length and a spin current, which is defined as $J_s(x) = J_{1=2}(x) - J_{1=2}(x) = \int_k (ek=m) S_{0;px}(x; k)$. It

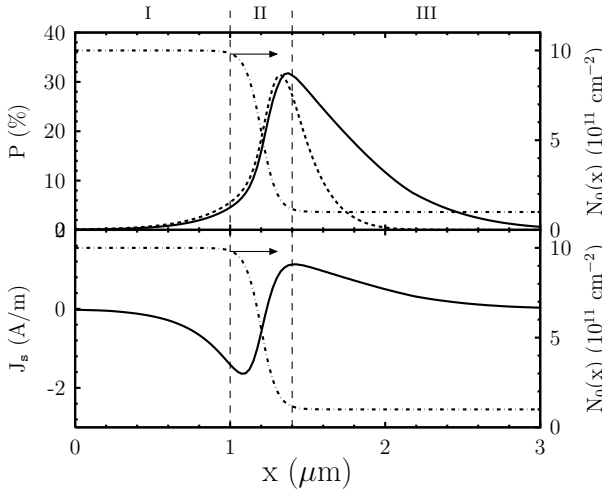


FIG. 2: The induced spin current and spin polarization in GaAs QW with a designed doping profile. The upper panel presents the spin polarization $P(x)$ in the QW, Dashed curve: with an uniform electrochemical potential (hence zero electric field in the uniform charge-density regions); Solid curve: with an additional applied voltage of 0.33 V that gives an electric field of 2 kV/cm in region III. The spin current density $J_s(x)$ for the applied voltage of 0.33 V is plotted as solid curve in the lower panel. The doping profile is plotted as dash-dotted curves in the figure with the scales on the right hand side of the figure. $T = 120$ K.

is noted that the spin current here is in fact the spin polarization carried by the charge current and therefore is parallel to the charge current. Therefore the device made from this effect is a two-terminal device. Moreover, as the components of the device are all semiconductors, the spin injection of this kind of devices does not suffer the obstacle of the conductance mismatch that has to be overcome in the spin injection from ferromagnetic metals to semiconductors [18, 19]. Therefore, one can achieve both large spin polarization and large spin current by the proposed device here. It is also worth to note that our simulation shows that the peak of induced spin polarization in the above device can achieve around 15 % at the room temperature. Therefore the spin generation in this kind of devices is very robust in most of the working conditions. The spatial distribution of the spin accumulation can be measured by spatiotemporal Kerr microscopy [20], while the spin current can be detected by building a light-emitting-diode next to region II or III and measuring the polarization of the electroluminescence spectra in the diode [21].

In conclusion, it is shown that the charge density gradient can induce a large spin polarization/current in the system with linear momentum-dependent spin-orbit coupling. As the charge gradient can be created and maintained through doping profile, the spin polarization induced by this charge gradient is very robust. This effect can be used to build two-terminal devices that generate

and inject spin polarized current with practical useful polarization non-magnetically. As the components of this kind of devices are all semiconductors, one can use the mature semiconductor production technology to achieve both large spin polarization and large spin current.

This work was supported by the Natural Science Foundation of China under Grant No. 90303012. MWW was also supported by the "100 Person Project" of Chinese Academy of Sciences and the Natural Science Foundation of China under Grant No. 10247002. MQW was partially supported by China Postdoctoral Science Foundation.

Author to whom correspondence should be addressed;
Electronic address: mwwu@ustc.edu.cn.

^y Mailing Address.

- [1] D. D. Awschalom, N. Samarth, and D. Loss, eds., *Semiconductor Spintronics and Quantum Computation* (Springer, Berlin, 2002).
- [2] I. Zutic, J. Fabian, and S. D. Samarth, *Rev. Mod. Phys.* **76**, 323 (2004).
- [3] S. D. Ganichev, E. L. Ivchenko, V. V. Bel'kov, S. A. Tarasenko, M. Sollinger, D. Weiss, W. Wegscheider, and W. Prettl, *Nature* **417**, 153 (2002).
- [4] S. D. Ganichev, P. Schneider, V. V. Bel'kov, E. L. Ivchenko, S. A. Tarasenko, W. Wegscheider, D. Weiss, D. Schuh, B. N. Murgan, P. J. Phillips, et al., *Phys. Rev. B* **68**, 081302(R) (2003).
- [5] S. A. Tarasenko, V. I. Perel', and I. N. Yassievich, *Phys. Rev. Lett.* **93**, 056601 (2004).
- [6] J. Sinova, D. Culcer, Q. Niu, N. A. Sinitsyn, T. Jungwirth, and A. H. MacDonald, *Phys. Rev. Lett.* **92**, 126603 (2004).
- [7] R. Raimondi and P. Schwab, cond-mat/0408233.
- [8] M. I. D'yakonov and V. I. Perel', *Zh. Eksp. Teor. Fiz.* **60**, 1954 (1971), [Sov. Phys. JETP **33**, 1053 (1971)].
- [9] G. D. Resselhaus, *Phys. Rev.* **100**, 580 (1955).
- [10] Y. A. Bychkov and E. I. Rashba, *J. Phys. C* **17**, 6039 (1984).
- [11] M. W. Wu and H. Metiu, *Phys. Rev. B* **61**, 2945 (2000).
- [12] M. W. Wu and C. Z. Ning, *phys. stat. sol. (b)* **222**, 523 (2000).
- [13] M. Q. Wang and M. W. Wu, *J. Appl. Phys.* **93**, 410 (2003).
- [14] F. M. Mier and B. P. Zakharchenya, eds., *Optical Orientation* (North-Holland, Amsterdam, 1984).
- [15] M. Q. Wang, M. W. Wu, and L. Jiang, *Phys. Rev. B* **69**, 245320 (2004).
- [16] M. Z. M. Jaije, E. A. de Andrade e Silva, and L. J. Sham, *Phys. Rev. B* **47**, 15776 (1993).
- [17] O. M. Adelung, M. Schultz, and H. Weiss, eds., *Numerical Data and Functional Relationships in Science and Technology*, Landolt-Bornstein, New Series, vol. 17 (Springer-Verlag, Berlin, 1982).
- [18] G. Schmidt, D. Ferrand, L. W. Molenkamp, A. T. Filip, and B. J. van Wees, *Phys. Rev. B* **62**, R4790 (2000).
- [19] E. I. Rashba, *Phys. Rev. B* **62**, R16267 (2000).
- [20] J. Stephens, J. Berezovsky, J. P. M. Guitre, L. J. Sham, A. C. Gossard, and D. D. Awschalom, *Phys. Rev. Lett.* **93**, 097602 (2004).

- [21] Y. Ohno, D. K. Young, B. Beschoten, F. Matsukura, H. Ohno, and D. D. Awschalom, *Nature* 402, 790 (1999).